Biosensors and Bioelectronics 41 (2013) 192–198

Contents lists available at SciVerse ScienceDirect

Biosensors and Bioelectronics

journal homepage: www.elsevier.com/locate/bios

# Electrochemical cell chip to detect environmental toxicants based on cell cycle arrest technique

Md. Abdul Kafi [a], Cheol-Heon Yea [b], Tae-Hyung Kim [b], Ajay Kumar Yagati [a], Jeong-Woo Choi [a,b,*]

[a] Interdisciplinary Program of Integrated Biotechnology, Sogang University, #1 Shinsu-Dong, Mapo-Gu, Seoul 121-742, Republic of Korea
[b] Department of Chemical & Biomolecular Engineering, Sogang University, #1 Shinsu-Dong, Mapo-Gu, Seoul 121-742, Republic of Korea

ARTICLE INFO

*Article history:*
Received 30 April 2012
Received in revised form
6 August 2012
Accepted 8 August 2012
Available online 18 August 2012

*Keywords:*
Cell-based biochip
Cell-cycle
Environmental toxicity
Cyclic voltammetry (CV)
Differential pulse voltammetry (DPV)

ABSTRACT

A cell-based chip was recently developed and shown to be an effective *in vitro* tool for analyzing effect of environmental toxin on target cells. However, common cell chips are inappropriate for the detection of multiple environmental toxins. Here, we fabricated a neural cell chip to detect different cellular responses induced by BPA (bisphenol-A) and PCB (poly chlorinated biphenyl). This approach was based on an electrochemical method using a cell cycle-arrest technique. Neural cells were synchronized at the synthesis phase by treatment with thymidine, which results in a sharp reduction peak when compared to unsynchronized cells. The fabricated chip containing 50% G1/S and 50% G2/M phase cells was used to determine the effects of environmental toxins on neural cancer cells. At the end, the cell-chips could be used to assess both BPA and PCB toxicity that the cells were completely synchronized at the G1/S and G2/M phase. The proposed neural cell chip can be a useful tool for biosensors to evaluate easily and sensitively multiple effects of environmental toxicants on target cells.



## 1. Introduction

Cell-based chips have a wide range of applications in the fields of pharmacology, medicine, cell biology, toxicology, basic neuroscience, and environmental monitoring (Bery and Grivell, 1995; Kafi et al., 2010a,b). Alterations in the cellular electro-dynamic systems provide information about the effect of a stimulus on living cells. Establishing a strong cell–substrate interaction is essential for obtaining proper functional information rather than analytical information. Several ECM (extracellular matrix) proteins or their functional components have been successfully used to establish a link between cells and electrodes. Bovine collagen, poly-l-lysine, RGD (Arg–Gly–Asp) peptide sequences are potential bioligands that can be used as a thin layer on metal electrode surface for enhanced cellular attachment (Dwyer et al., 1999; Pierschbacher and Ruoslahti, 1984).

We recently developed a cell chip technology that was capable of effectively measuring changes in cell viability upon exposure to different kinds of environmental toxins (Kafi et al., 2010a,b) or anticancer drugs (El-Said et al., 2009), and this approach is based on simple and rapid electrochemical techniques. These electrochemical methods have also been incorporated to cell-based sensor arrays as well as to electrical sensing devices for the detection of signal-frequency patterns produced by cells in growth media (Choi et al., 2004; May et al., 2004; Yea et al., 2007). These whole cell-based sensing systems employ sensor cells that electro-physiologic state varies upon exposure to toxic substances. The cells added toxin produce readily measurable differences in signal intensities and can be used as new tools for cell viability measurements (Kafi et al., 2011a,b,c, 2010a,b). These whole cell-based sensing systems enable monitoring the environmental state whether the specific environmental toxin exists in the experimental condition. However, electrochemical techniques based on real-time monitoring chips that can assess the effects of a mixture of toxins have not yet been developed.

In a previous study, we found that the redox phenomenon at the cell-electrode interface is critical for detecting the electrochemical characteristics of target cells, which vary depending on the cell line (Kafi et al., 2011a, 2010a,b). Recently, we observed that the electrochemical properties of each cell depend on the cell cycle stage, which has been used as a label-free technology for cell cycle monitoring (Kafi et al., 2011b). Cells tend to show cycle-dependent characteristics, which are defined by a sequence of events in which several specific nuclear changes occur. Based on morphological changes that occur during mammalian cell division, the cell cycle can be broadly subdivided into inter-phase and mitotic (M)-phase stages (Alberts et al., 2002). Inter-phase encompasses the G1, S, and G2-phases. G1-phase is the first pause, in which cells prepare for DNA synthesis and prevent replication errors. In the S-phase, cells synthesize DNA and thus have aneuploidic DNA content between 2*N* and 4*N* (Nelson et al., 2002). Conversely, G2-phase is the second

* Corresponding author at: Department of Chemical & Biomolecular Engineering, Sogang University, #1 Shinsu-Dong, Mapo-Gu, Seoul 121-742, Republic of Korea. Tel.: +82 2 705 8480; fax: +82 2 3273 0331.
*E-mail addresses:* jwchoi@ccs.sogang.ac.kr, jwchoi@sogang.ac.kr (J.-W. Choi).

0956-5663/$ - see front matter © 2012 Elsevier B.V. All rights reserved.
http://dx.doi.org/10.1016/j.bios.2012.08.023

pause of the cell cycle, in which the cells prepare for mitosis (M-phase) and protect against mitotic error. The M-phase contains several sub-phases, including prophase, metaphase, anaphase, and telophase, causing cytokinesis to form daughter cells (Alberts et al., 2002). Based on these numerous cytological changes, the M-phase and S-phase are most vulnerable to environmental or endogenous stimulation, which might be used as an environmental switch, i.e. it could be turned on in the presence of toxins or stressful conditions. We previously examined phase specific electrochemical signals from the G1/S and G2/M phases of a cell cycle (Kafi et al., 2011b). Based on this previous work, we hypothesized that multiple environmental toxins can be monitored using electrochemical techniques by exploiting phase specific changes in cells.

Here, we suggest that an innovative PLL (poly-L-lysine) based biochip, on which neural cells were immobilized and artificial synchronization was achieved for electrochemical monitoring of the phase specific cytotoxicity of PCB and bisphenol-A. The cells on the electrode surface were synchronized in the G1/S and G2/M-phase using thymidine and nocodazole (Gutierrez et al., 2010). Successful synchronization was confirmed by FACS (Fluorescence activated cell sorting), Western blot, and electrochemical analysis. The phase specific electrical current generated by the toxin treated cells was then detected and analyzed.

## 2. Materials and methods

### 2.1. Chemicals

Thymidine and nocodazole were purchased from Sigma and used without further purification. PLL was purchased from Biomedical Technologies (Stoughton, USA). 2,2′, 4,4′, 5,5′-6 hexachlorobiphenyl (PCB 153) was purchased from AccuStandard®, Inc., USA. Bisphenol-A was purchased from Sigma Aldrich. RPMI 1640 Medium (RPMI 1640, purchased from Fresh media®, Daegu, 704-230, South Korea), fetal bovine serum (FBS), antibiotics (penicillin–streptomycin, 10,000 U/ml of penicillin sodium, and 10,000 μg/ml of streptomycin sulfate in 0.83% saline), and trypsin (0.05% trypsin, 0.53 mM EDTA-4Na) were obtained from Gibco (Invitrogen, Grand Island, USA). Phosphate buffered saline (PBS) (pH 7.4, 10 mM) was purchased from Sigma-Aldrich (St. Louis, MO, USA). Other chemicals were all of analytical grade. All solutions were prepared with double-distilled water, which was purified using a Milli-Q purification system (Branstead) to a specific resistance of $>18$ MΩ cm.

### 2.2. Preparation of PLL modified electrode

A smooth gold surface is important to support efficient peptide binding (Lee et al., 2011, 2010). For this, a silicon-based gold electrode was first cleaned with a freshly prepared piranha solution (1:3 mixture of 30% $H_2O_2$ and concentrated $H_2SO_4$) for 5 min and then rinsed thoroughly with double-distilled water. The electrode was electrochemically cleaned in 0.5 M $H_2SO_4$ at a scan rate of 0.2 V/s over potential range from 0.8 V to $-0.2$ V until constant cyclic voltammograms were obtained. The electrode was then dried with purified nitrogen. After the pretreatment step, the electrode was placed in 1 mg/mL MUA (Mercapto undecanoic acid) suspension for 30 min to allow for the formation of a self-assembled MUA layer on the gold surface. The surface was then washed with DW (Deionized water) and dried (this modified electrode is denoted as Au/MUA). 0.1 mg/mL PLL was placed on the Au/MUA surface and incubated overnight, resulting in the incorporation of a positive group ($-NH_2$) on the electrode. The electrode was then thoroughly rinsed with DW to remove loosely bound peptide, and subsequently air-dried (this modified electrode is denoted as Au/MUA/PLL). All steps during the preparation of the samples for AFM (Atomic force microscopy) characterization were repeated on smooth gold sheets.

### 2.3. Chip design and cell immobilization

For the electrochemical measurements, a 2 cm × 1 cm × 0.5 cm (width × length × height) cell chip chamber was fabricated by fixing a plastic chamber (Lab-Tek(R), Thermo fisher scientific, USA) to the Au/MUA/PLL working electrode using PDMS (Polydimethylsiloxane), which produced an exposure area of approximately 2 cm × 1 cm. Rat pheochromocytoma (PC12) cells were then seeded on the electrode at a density of $3.5 \times 10^5$ cells/chip and immobilized via electrostatic interactions for 24 h in a standard cell culture environment (this modified electrode is denoted as Au/MUA/PLL/Cell) (Fig. 1b).

### 2.4. Cell synchronization

Artificial synchronization was achieved as described previously (Kafi et al., 2011b). Briefly, the Au/MUA/PLL/Cell electrode

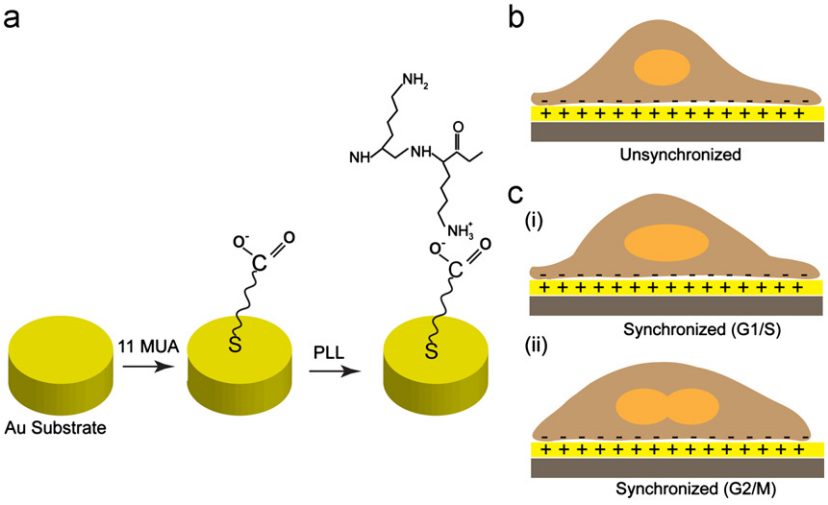


**Fig. 1.** Schematic of the step-by-step modification of the chip surface: (a) PLL immobilized on MUA functionalized Au surface, (b) unsynchronized cell immobilized electrostatically on the functionalized Au surface and (c) cell synchronized at G1/S (i) and G2/M phase (ii).

was treated with 2 mM thymidine in culture medium (RPMI 1640) for 18 h, followed by an 8 h release in fresh medium, and then again with 2 mM thymidine for another 18 h to block cells in the G1/S-phase (known as double thymidine mediated G1/S block). Similarly, another Au/MUA/PLL/Cell electrode was treated initially with 2 mM thymidine as mentioned before for 18 h, followed by a 4 h release in fresh medium, and then with 100 ng/mL of nocodazole for another 10 h to block the cells in the G2/M-phase (known as thymidine-nocodazole mediated G2/M block). Thus, the working electrodes were prepared for electrochemical analysis of the cytotoxicity of BPA and PCB at different phases in the cell cycle. Furthermore, the G1/S synchronized chip was released in fresh medium for 6 h to obtain 50% G1/S and 50% G2/M on the same chip, which was then used for real-time analysis of mixtures of PCB and BPA.

### 2.5. Electrochemical measurements

Cyclic voltammogram (CV) and differential pulse voltammogram (DPV) measurements were carried out with a CHI660C Potentiostat (CH Instruments). The commonly used three-electrode configuration was employed for the electrochemical measurements (Kafi et al., 2011a,b,c), where the fabricated cell based Au electrode served as the working electrode and Ag/AgCl and Pt served as the reference and counter electrode, respectively. Prior to the electrochemical measurements, a gold electrode with cells was washed twice with 10 mM PBS buffer (pH 7.4). Finally, electrochemical measurements were performed using 2 mL of the same PBS solution as the electrolyte. All measurements were performed independently at least three times, and error bars are shown in the figures.

### 2.6. Fluorescence-activated cells sorting (FACS) analysis

Cells were washed once with ice-cold phosphate-buffered saline (PBS) and resuspended in 100 μL of ice-cold PBS. 900 μL cold methanol was then added to the cells, mixed gently, and incubated on ice or in a −20 °C freezer for at least 30 min. Cells were washed once with PBS and resuspended in 500 μL PBS. RNAse (100 μg/mL) was added and incubated with the samples at room temperature for 60 min. The resulting cell pellets were re-suspended in 0.5 mL of PBS containing 50 μg/mL of propidium iodide (Sigma-Aldrich Chemical Co., St. Louis, MO) and 100 μg/mL of RNase (Invitrogen, Carlsbad, CA), followed by incubation at 37 °C for 30 min. Cell-cycle distribution was examined by measuring the DNA content using a flow cytometer (FACScan, Becton Dickinson, San Jose, CA), as described previously (Zhu et al., 2000). A minimum of $10^4$ cells per data point was analyzed. The regions marked M1, M2, and M3 represent the G1, S, and G2/M-phase of the cell cycle, respectively (Fig. 3d-iii).

### 2.7. Protein assay

The cell pellet obtained from centrifugation (1000*g*) was solubilized for 15 min at 4 °C in lysis buffer. Cell lysates were centrifuged at 13,000*g* for 30 min at 4 °C and supernatant was then collected. The BCA protein assay reagent (Pierce Chemicals) was used to determine protein concentration. SDS-polyacrylamide gels (12% for actin and cycline B1, 16% for p-HH$^3$) were prepared to separate protein samples (25 μg each) by electrophoresis and then transferred onto polyvinylidene difluoride membranes (Bio-Rad). The membranes were then probed with anti-p-HH$^3$ (1:2000; cell signaling), anti-cycline B1 (1:2000; Abchem), cyclin E (1:200; Santa Cruz Biotechnology, Inc.) and anti-β-actin (A-5441, 1:10,000) and incubated overnight at 4 °C. The membranes were then washed thrice with PBS containing 0.015% (vol/vol) Tween-20 for 10 min each and incubated with secondary antibody (anti-mouse IgG-HRP for actin, anti-rabbit IgG-HRP for cycline B1 and p-HH$^3$) for 1 h at room temperature. Finally, the membranes were washed again thrice before being developed using enhanced chemiluminescence (Amersham Biosciences, Uppsala, Sweden).

### 2.8. Data analysis

The height of the cathodic peaks ($I_{pc}$) in the cyclic voltammogram and the differential pulsed voltammogram were used for quantitative analysis. Data were analyzed using the computerized statistical program "Origin 8". Data are expressed as mean ± SE ($N=3$). Significant differences were determined for $p < 0.05$.

## 3. Results and discussion

### 3.1. Step-by-step fabrication of the chip

The step-by-step fabrication process for the cell-attaching electrode used in the cell chip is illustrated in Fig. 1. The Au electrode needs to be functionalized with positively charged ECM materials or its components for effective cell immobilization (Kafi et al., 2011a, 2010a,b). In the present study, a nano-scaled PLL layer was placed on the MUA functionalized Au surface (Fig. 1a). MUA containing a thiol residue on its terminus were self-assembled on the Au electrode via an Au–S covalent bond, and the carboxyl group on the other terminus was used to form electrostatic bonds between the $NH_2$ of PLL, resulting in a positively charged Au surface, which is needed for strong attachment of cells to the electrode surface (Jin and Lee, 2006; Kafi et al., 2010a). Positively charged PLL-modified Au surfaces have been

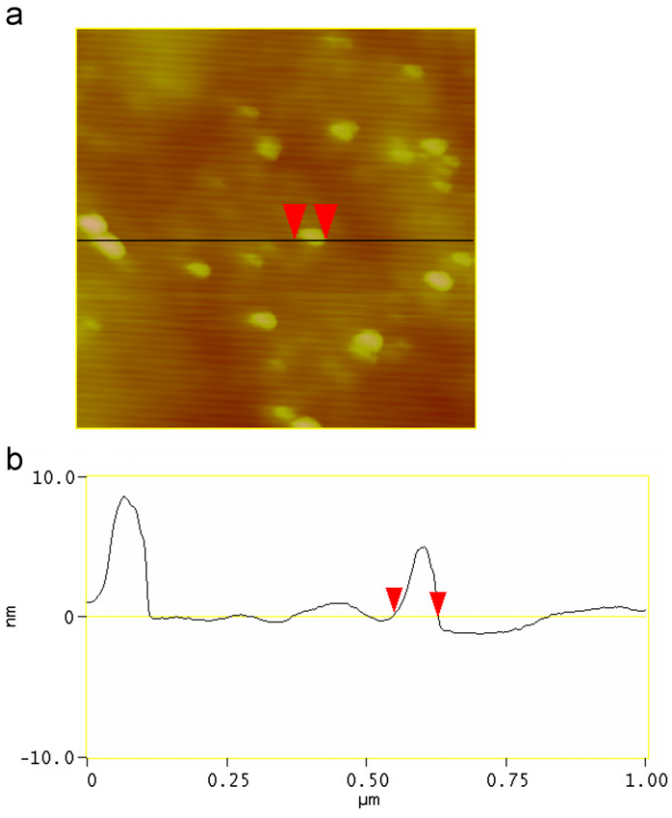


**Fig. 2.** (a) AFM images of the fabricated PLL dots on the Au surface. (b) Profiles shown below indicate that the PLL dots on the Au surface are 78 nm in size. The images were scanned at a rate of 1 Hz and the image size is 1 μm.

shown to result in strong electrostatic interactions with the negatively charged surface of cells (Kafi et al., 2010a; Ruoslahti, 1996). The enhanced binding affinities of the negatively charged cell membrane to the positively charged electrode surface prevent cell detachment caused by washing throughout the experiment, and they also enhance electron transfer during the electrochemical measurements (Kafi et al., 2010a). The cell based electrodes were then subjected to double thymidine (*T/T*) treatment, which converted the cells to the G1/S-phase (Fig. 1c-i). Similarly, cells were arrested in the G2/M-phase by thymidine/nocodazole treatment, as shown in our previous study (Kafi et al., 2011b) (Fig. 1c-ii). These electrodes showed different electrochemical characteristics depending on whether the cells were in the G1/S, G2/M, or unsynchronized phase and these differences were used to monitor changes in the response to toxin exposure based on the intensity or potential difference in the voltammetry.

### 3.2. Surface topographic characterization of the PLL modified electrode by AFM

The surface topography of the PLL modified Au substrate was investigated with AFM (SPM Multimode, Veeco, USA) in tapping mode at room temperature under ambient air. AFM images were acquired at a scan rate of 2.0 Hz using a phosphorous (*n*) doped silicon cantilever. The spontaneous formation of a self-assembled monolayer of PLL dots on polycrystalline gold was achieved by dipping the substrate into a solution with the corresponding concentrations (Fig. 2a). The section analysis of the acquired AFM images demonstrated that the PLL dots were 78 nm in size and were homogenously distributed throughout the Au surface (Fig. 2b). These results indicate that the PLL-dots were formed on an Au surface via self-assembly using MUA intermediate layer. The formation of PLL dots on a Au substrate has been reported to improve cell adhesion strength as well as cell viability (Choi et al., 2007).

### 3.3. Electrochemical characterizations of fabricated cell chip

Fig. 3a showed voltammetric signals obtained at various steps of surface modification during the fabrication of the cell chip, where very weak and/or no signal were obtained from bare Au and Au/PLL electrode and distinct redox peaks appeared after cell immobilization. The strong reduction peak at +20 mV and oxidation peak at +390 mV, which is the typical redox property of PC12 cells (Kafi et al., 2010a), was recorded for unsynchronized cell (Fig. 3a). However, double thymidine induced G1/S synchronized chip resulted in two sets of redox peaks (Fig. 3b), a sharp reduction appeared at −30 mV leaving another wide reduction at +210 mV with the corresponding oxidation peaks at +90 mV and +430 mV, which were different from that of the unsynchronized cells showed in Fig. 3a. These differences in CV signaling from identical cells in different phases (G1/S, G2/M) may have been due to changes in the redox properties of morphologically-altered cells (Mitchison and Salmon, 2001). The sharp peak observed at +20 mV was previously reported to be due to G1/S

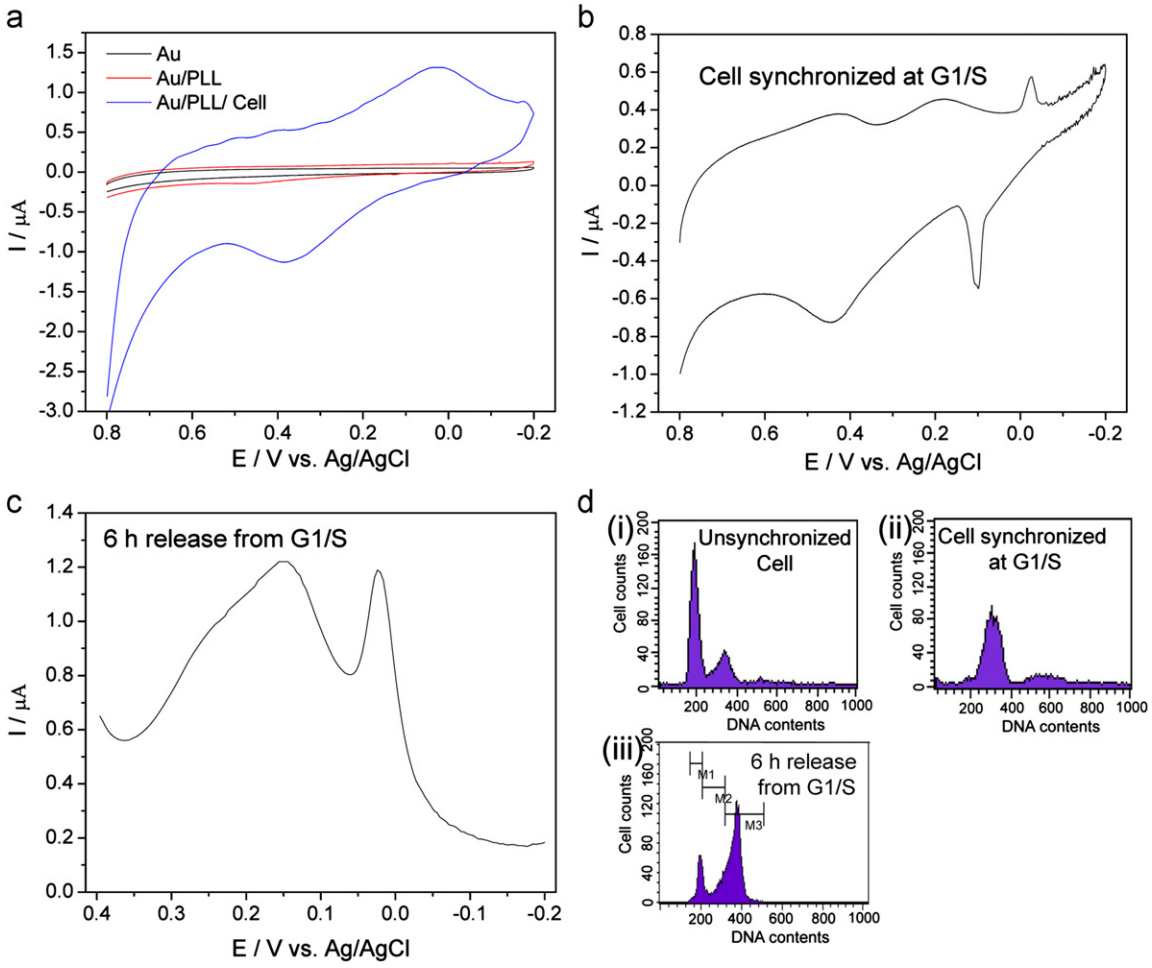


**Fig. 3.** (a) Cyclic voltammograms of the step-by-step fabrication of the PLL based cell chip, (b) cyclic voltammogram obtained after the cells were synchronized at G1/S, (c) two distinct DPV peak from cells 6 h after release from G1/S and (d) confirmation of the above synchronization by FACS.

cells (Kafi et al., 2011b). Fig. 3c showed the DPV signal obtained from G1/S cells released for 6 h. 50% of the cells moved to the G2/M phase, which produced nearly the same peak intensities in different potentials (Kafi et al., 2011b). These results are consistent with our previous study, where we reported that cells in the G1/S-phase produced a sharp peak at a potential of −30 mV, but G2/M-phase shifted the peak of −30 mV to +30 mV and produced an another peak at +150 mV, which increased with time after release from the double thymidine treatment (Kafi et al., 2011b). Furthermore, the synchronized PC12 cells used in the above experiments were confirmed by FACS (Fig. 3d), which showed that approximately 75% of the cells were fixed in G1/S-phase when treated with double thymidine (Fig. 3d-ii). In contrast, 50% of the cells were either in the G1/S or G2/M-phase when the G1/S block chip was released for 6 h (Fig. 3d-iii). These features of the synchronized cells were found to differ from those of the unsynchronized group, which consisted of a mixture of cells in different phases of the cell cycle (Fig. 3d-i). This indicates successful synchronization of the cells on the chip. The chip containing cells in both the G1/S and G2/M phase was achieved 6 h after release from the G1/S phase, which produced two peaks at different potentials. These peaks could be used to assess the phase specific toxicity of mixed environmental samples.

### 3.4. Monitoring of cell cycle specific neurotoxicity of PCB and BPA

After confirmation of cell cycle arrest using conventional methods, the chip containing cells in both the G1/S and G2/M-phase were treated with PCB and/or BPA and changes in the electrochemical signals were measured. Fig. 4a shows that the G1/S peaks sharply decreased after 500 nM BPA treatment and the G2/M peak remained intact. However, the peak corresponding to G2/M decreased when the chip was treated with 50 nM PCB and no effect was observed on the G1/S peak (Fig. 4b). These

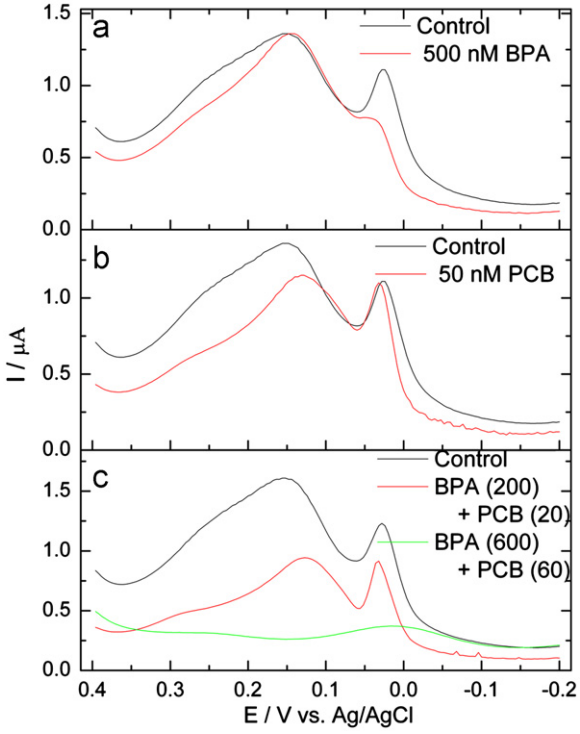


**Fig. 4.** Phase specific toxicities of BPA and PCB were analyzed based on the two peaks obtained from cells 6 h released from G1/S, (a) shows BPA toxicity mostly affects the G1/S peak whereas (b) PCB mostly affect the G2/M peak. However, (c) both peaks decreased when the chip was treated with a mixture of both toxins and no peak was observed when a high concentration of toxin was used.

results suggested that BPA affects cells in the G1/S phase and PCB affects cells in the G2/M phase. In addition, both peaks decreased when a mixture of low concentrations (200 nM BPA and 20 nM PCB) of both toxins was added. Moreover, no peak was detected when a high concentration of the mixed toxin (600 nM BPA and 60 nM PCB) was added, which indicates that all the cells had died and were washed off the electrode (Fig. 4c). The neurotoxic doses of BPA and PCB were in agreement with a previous study (Kafi et al., 2011a, 2010a,b), which reported that 150 nM BPA and 20 nM PCB were toxic to PC12 cells. It is well known that release from the G1/S block allows cells to progress into the M-phase for nuclear division and cell division (Jin and Lee, 2006). During this phase, cells pass through a number of complex processes, including prophase, prometaphase, metaphase, anaphase, and telophase that lead to several changes in the nucleus (Cude et al., 2007; Huang et al., 2001). These cytological changes might be responsible for the varying susceptibility to PCB and BPA at different phases of a cycle. Therefore, the decreased phase specific electrochemical signal was likely caused by the toxin used in this study. So, analysis and quantification of the current peak obtained from DPV signal intensities can be used to indirectly but accurately determine the effect of a toxicant dose on completely synchronized cells.

### 3.5. Confirmation of complete synchronization of cells on chip at G1/S and G2/M

To accurately assess the effect of a toxicant dose using the current peaks obtained from the cellular DPV signal intensities, complete synchronization using our newly developed electrochemical method is needed. Therefore, in this experiment, PC-12 cells were completely synchronized at the G1/S and G2/M using thymidine and/or nocodazole treatment according to the protocol described in our previous study (Kafi et al., 2011b). On-chip synchronization of PC12 cells was confirmed by Western blot analysis of the phase-specific proteins cyclin B1, Cyclin E, and pHH$^3$. Fig. 5a shows that p-HH$^3$ was expressed in the G2/M-phase but not in the unsynchronized and G1/S-blocked cells, whereas cyclin B1 was predominantly expressed in G1/S-phase cells (Cogswell et al., 1995; Pines and Hunter, 1989). In contrast, cyclin E was predominantly expressed in G1/S and G2/M blocked cells. These results demonstrated that the cells were successfully synchronized on the chip. These cell cycle blocks were further confirmed using our recently developed electrochemical method, which produces distinct phase specific DPV signals from double thymidine induced G1/S (Fig. 5b) and thymidine Nocodazole induced G2/M (Fig. 5c) relative to the unsynchronized control cells (Fig. 5d). Therefore, the artificial cell cycle arrest on the chip was shown to be successful by both western blot and the electrochemical method.

### 3.6. Dose-dependent PCB and BPA toxicity assay on completely synchronized cell

After confirming complete synchronization of cells at G1/S and G2/M phases, the chips were exposed to different concentrations of PCB and BPA and cell viability was measured. For effective toxicity measurements, the cells, $3.5 \times 10^5$ cells/ml, were synchronized on each chip because high density of cells is not suitable for proper synchronization and electrochemical measurements (Kafi et al., 2011b). Prior to recording the DPV current responses, G2/M phase synchronized cells were exposed to several concentrations of PCB and G2/M phase synchronized cells were exposed to several concentration of BPA. Fig. 6a shows the current responses from G2/M cells exposed to various PCB concentrations (20–120 nM). A dose dependent decrease in DPV current signals was recorded as functions of PCB concentrations

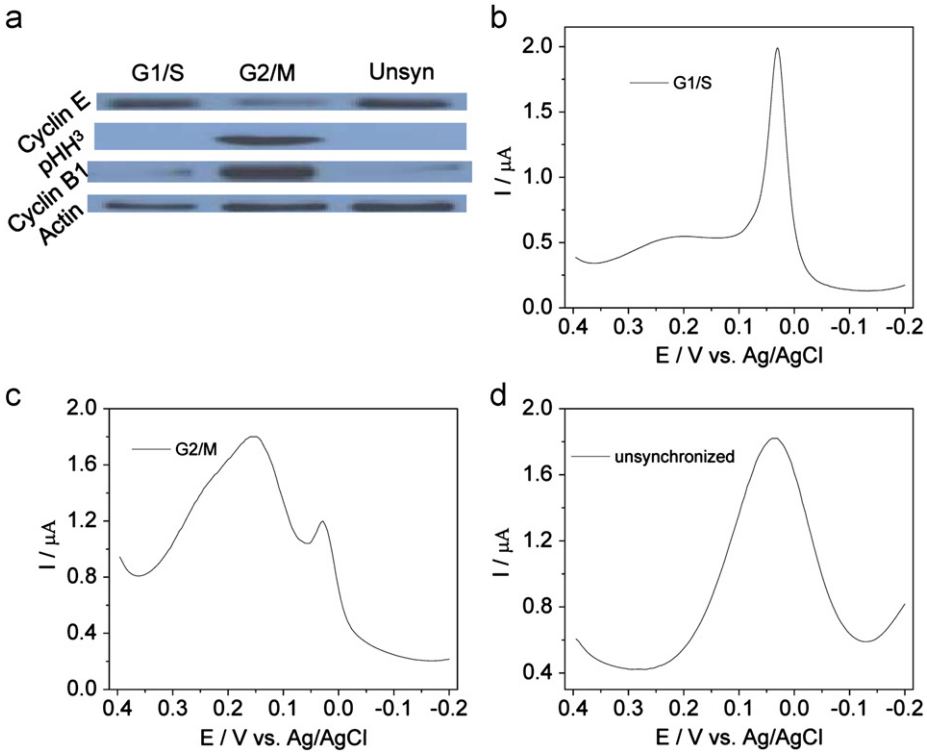


**Fig. 5.** Confirmation of complete synchronization: (a) Western blot and (b–d) electrochemical method for the confirmation cell synchronized at G1/S and G2/M.

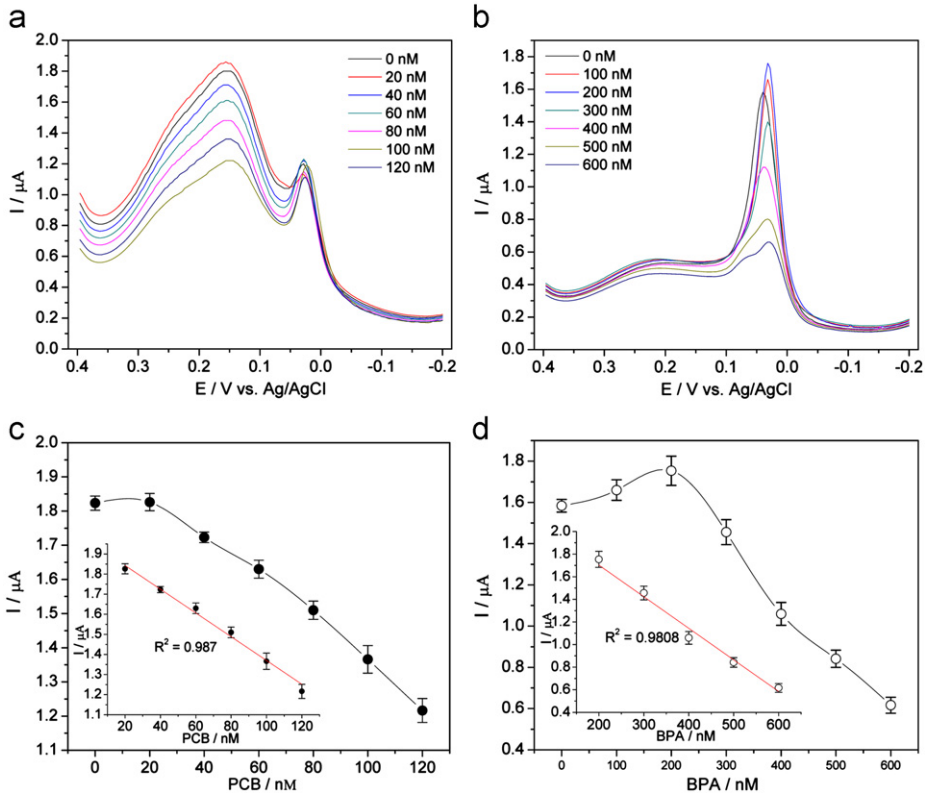


**Fig. 6.** Concentration dependent cyto-toxicity; (a) effect of PCB on cells completely synchronized at G2/M phase and (b) effect of BPA on cells completely synchronized at G1/S phase. Dose response curve obtained from PCB treatment on G2/M synchronized chip (c) and BPA treatment on G1/S synchronized chip (d).

(Fig. 6c). The current peaks at the initial concentration (20 nM) remained unchanged when comparing with the non treated control, indicating a sub-toxic dose. However, the reduction peak showed a negative linear correlation ($R^2$ = 0.987) when cells were exposed to 40–120 nM of PCB (Fig. 6b inset), which indicates cytotoxicity. We previously reported that electrochemical signals have positive linear correlations with the concentration of viable cells; therefore, a decrease in the signal after treatment with the

toxicant can be attributed to a loss of cell viability (Kafi et al., 2011a, 2010a,b; Woolley et al., 2002; Yilmaz et al., 2006). Similarly, the current responses from G1/S cells exposed to BPA are plotted in Fig. 6b, which was different from the response observed for other toxicants; BPA showed a dose dependent dual effect (Kafi et al., 2011a). The current peaks increased when treated with BPA at concentrations between 100 nM and 200 nM BPA and decreased at higher concentrations (Fig. 6d). The reduction peak showed a negative linear correlation ($R^2=0.980$) when cells were exposed to 400–600 nM of BPA (Fig. 6d inset). This finding is in complete agreement with our previous report, where BPA toxicity was analyzed on unsynchronized cells (Kafi et al., 2011a). In the present study, we observed a similar dose effect of PCB and BPA on PC12 cell but this effect was different between G1/S and G2/M synchronized cells, which confirmed that PCB affects mitotic and short resting phase (G2) of the cell cycle and BPA affects the synthesis phase and large resting phase (G1). Therefore, we can conclude that cells in different phases of their cycle can be susceptible to different environmental toxins. The results of this study demonstrate that the effect of mixed toxins from environmental sources can be accurately measured using the developed synchronized cell based chip.

## 4. Conclusions

In this study, we developed a novel electrochemical detection method that uses cell cycle specific effects to detect PCB and BPA neurotoxins through cell chip technology. PC12 cells were immobilized on the PLL-modified chip surface and synchronized at G1/S. The cells were then released from this stage for 6 h. This process produced a two phase specific DPV signal and 50% of the cells were shown to be either in the G1/S or G2/M phase. The phase specific electrochemical signals displayed a different response when treated with PCB and BPA. We found that the G1/S peak was susceptible to BPA treatment and the G2/M peak was susceptible to PCB treatment. The phenomena indicate that BPA toxicity is related to the synthesis and large gap phase, whereas PCB toxicity is related to mitosis and short gape of the cell cycle. The cell chip containing cells completely synchronized to the G1/S and G2/M-phase was then exposed to varying concentrations of PCB and BPA and the effect of different treatment doses on cytotoxicity was measured, where differences at $\geq$20 nM PCB and $\geq$300 nM BPA were observed. Based on these results it was concluded that BPA was less toxic then PCB. The phase specific DPV signals were used as indicators to examine environmental toxins that have a significant effect on different phases of the cell. This new label-free method enables simple, easy, and rapid electrochemical analysis of the specific neurotoxins from a mixture of toxicants. The technology can be applied to the toxicity assessment of a specific toxicant from a bulk environmental sample, since cells in different phases of the cell cycle can behave differently even under same environmental samples.

## Acknowledgments

This work was supported by the National Research Foundation of Korea (NRF) grant funded by the Korea government (MEST) (2012-0000163), by the Nano/Bio Science & Technology Program (M10536090001-05N3609-00110) of the Ministry of Education, Science, and Technology (MEST), and by the Ministry of Knowledge Economy (MKE) and Korea Institute for Advancement in Technology (KIAT) through the Workforce Development Program in Strategic Technology.

## References

Alberts, B., Johnson, A., Lewis, J., Raff, M., Roberts, K., Walter, P., 2002. The Molecular Biology of the Cell. Garland Science Taylor & Fransis Group, New York.
Bery, M.N., Grivell, M.B., 1995. In: Walz, D., Berry, H., Milazzo, G. (Eds.), Bioelectrochemistry of Cells and Tissues. Birkhauser, Basel, Verlag. (pp. 134–158).
Choi, J.W., Nam, Y.S., Fujihira, M., 2004. Biotechnology and Bioprocess Engineering 9, 76–85.
Choi, J., Kim, M., Park, J., Jeon, J., Kim, D., Towns, A., 2007. Fibers and Polymers 8, 37–42.
Cogswell, J.P., Godlevski, M.M., Bonham, M., Bisi, J., Babiss, L., 1995. Molecular and Cell Biology 15, 2782–2790.
Cude, K., Wang, Y., Choi, H.J., Hsuan, S.L., Zhang, H., Wang, C.Y., Xia, Z., 2007. Journal of Cell Biology 177, 253–264.
Dwyer, D.S., Liu, Y., Bradley, R.J., 1999. Journal of Cellular Physiology 178, 93–101.
El-Said, W.A., Yea, C.H., Kwon, I.-K., Choi, J.-W., 2009. Biochip Journal 3, 105–112.
Gutierrez, G.J., Tsuj, T., Cross, J.V., Davis, R.J., Templeton, D.J., Jiang, W., Ronai, Z.A., 2010. Journal of Biological Chemistry 285, 14217–14228.
Huang, J.N., Park, I., Ellingson, E., Littlepage, L.E., Pellman, D., 2001. Journal of Cell Biology 154, 85–94.
Jin, H.S., Lee, T.H., 2006. Biochemical Journal 399, 335–342.
Kafi, M.A., Kim, T.-H., An, J.H., Choi, J.-W., 2011b. Analytical Chemistry 83, 2104–2111.
Kafi, M.A., Kim, T.-H., An, J.H., Choi, J.-W., 2011a. Biosensors and Bioelectronics 26, 3371–3375.
Kafi, M.A., Kim, T.-H., An, J.H., Kim, H., Choi, J.-W., 2011c. Sensor Letters l (9), 147–151.
Kafi, M.A., Kim, T.-H., Yagati, A.K., Kim, H., Choi, J.-W., 2010b. Biotechnology Letters 32, 1797–1802.
Kafi, M.A., Kim, T.-H., Yea, C.-H., Kim, H., Choi, J.-W., 2010a. Biosensors and Bioelectronics 26, 1359–1365.
Lee, T., Min, J., Kim, S.-U., Choi, J.-W., 2011. Biomaterials 32, 3815–3821.
Lee, T., Kim, S.-U., Min, J., Choi, J.-W., 2010. Advanced Materials 22, 510–514.
May, K.M., Wang, Y., Bachas, L.G., Anderson, K.W., 2004. Analytical Chemistry 76, 4156.
Mitchison, T.J., Salmon, E.D., 2001. Nature Cell Biology 3, E17–E21, http://dx.doi.org/10.1038/35050656.
Nelson, D.M., Ye, X., Hall, C., Santos, H., Ma, T., Kao, G.D., Yen, T.J., Harper, J.W., Adams, P.D., 2002. Molecular and Cellular Biology 22, 7459–7472.
Pierschbacher, M.D., Ruoslahti, E., 1984. Nature 309, 30–33.
Pines, J., Hunter, T., 1989. Cell 58, 833–846.
Ruoslahti, E., 1996. Annual Review of Cell and Developmental Biology 12, 697–715.
Woolley, D.E., Tetlow, L.C., Adlam, D.J., Gearey, D., Eden, R.D., Ward, T.H., Allen, T.D., 2002. Experimental Cell Research 273, 65–72.
Yea, C.H., Min, J., Choi, J.W., 2007. Biochip Journal 1, 219–227.
Yilmaz, B., Sandal, S., Chen, C., Carpenter, D.O., 2006. Toxicology 217, 184–193.
Zhu, H., Boobis, A.R., Gooderham, N.J., 2000. Cancer Research 60, 1283–1289.